

Long-term Monitoring of the Hwamyung Cable-Stayed Bridge using Wireless Sensor Network

*Khac-Duy Nguyen¹⁾, Jeong-Tae Kim²⁾, Sung Woo Shin³⁾, Chung-Bang
Yun⁴⁾
and Masanobu Shinozuka⁵⁾

^{1), 2)} *Department of Ocean Engineering, Pukyong National University, Busan 608-737,
Korea*

³⁾ *Department of Safety Engineering, Pukyong National University, Busan 608-739,
Korea*

⁴⁾ *School of Urban and Environmental Engineering, UNIST, Ulsan 689-798, Korea*

⁵⁾ *Department of Civil and Environmental Engineering, University of California, Irvine,
Irvine, CA 92697-2175, USA*

²⁾ *idis@pknu.ac.kr*

ABSTRACT

The technology of wireless sensor networks (WSNs) is innovative for structural health monitoring (SHM) of bridges. The installation time and implementation cost of the SHM system are greatly reduced by the adoption of WSN. This paper presents the long-term monitoring of a cable-stayed bridge (the Hwamyung Bridge) in Korea using Imote2-platformed WSN. First, the wireless monitoring system of the bridge is briefly described. Next, modal parameters of the bridge and cable forces of several selected cables were estimated from the acceleration signals measured by the WSN. Then the effects of environmental and loading factors on the bridge's characteristics were experimentally investigated. Those factors include temperature variation, wind and typhoon, and asphalt paving installation.

1. INTRODUCTION

Over the two past decades, structural health monitoring (SHM) has become increasingly important for assessing the safety and remaining service life of civil infrastructures. In order to secure the structural integrity, many robust sensing technologies and SHM methods have been developed (Doebbling et al. 1998, Sohn et al. 2003, Kim et al. 2010). Recently, the interest on the safety assessment of cable-stayed bridges has been increasing (Spencer and Cho 2011). For a cable-stayed bridge, critical damage may be occurred in main structural components such as deck, cable, and pylon by resulting in stiffness-loss, crack growth, concrete degradation, etc. Critical

damage in cable-anchorage subsystem may include cable force loss, anchorage damage and anchorage force loss.

Conventional SHM systems mainly requires a number of sensors, a huge amount of signal transmitting wires, data acquisition instruments and centralized data storage servers. Therefore, the cost associated with installation and maintenance of the SHM systems is very high. Recently, low-cost, stand-alone, smart sensors have been developed for SHM by many research groups. Straser and Kiremidjian (1998) first proposed a design of a low-cost wireless modular monitoring system for SHM applications. Since then, many researchers have developed wireless sensors based on a variety of sensor platforms (Lynch et al. 2006, Mascarenas et al. 2007, Rice et al. 2010, Spencer and Cho 2011, Kim et al. 2011). By adopting those smart sensors for SHM in large structures, the costs are greatly reduced and the data processing and information management will be very effective by ways of sensing and on-board computation, wireless transmission, and green energy harvesting.

In this paper, a long-term monitoring of the Hwamyung cable-stayed Bridge in Korea using Imote2-platformed WSN is presented. First, the wireless monitoring system of the bridge is briefly described. Next, modal parameters of the bridge and cable forces of several selected cables were estimated from the acceleration signals measured by the WSN. Then the effects of environmental and loading factors on the bridge characteristics were experimentally investigated. Those factors include temperature variation, wind and typhoon, and asphalt paving installation.

2. DEPLOYMENT OF WIRELESS SENSOR NETWORK

A field test was conducted on the Hwamyung cable-stayed Bridge crossing Nakdong river between Busan and Gimhae, Korea, as shown in Fig. 3. The bridge was constructed by Hyundai Engineering & Construction Co., Ltd., from December 2004 to July 2012. The test history on the bridge is summarized in Table 1. The project on monitoring of the Hwamyung Bridge started from May 2011. Since then, there has been four work phases: design of sensor system, sensor system setup, performance evaluation, and long-term monitoring.

For the sensor design phase, the hardware components of vibration nodes as well as the operation software for the sensors were designed. For the sensor system setup phase, the sensor system was deployed on the bridge by 21st June, 2011, and the internet-based remote monitoring system was set-up by the same period. For the performance evaluation phase, performance of the sensor system was evaluated with respect to wireless communication, energy harvesting, and signal measurement. For the long-term monitoring phase, several tasks have been performed, including monitoring of cable under temperature variation, investigating effect of typhoon on bridge behavior and investigating effect of dead load variation on bridge characteristics. During the monitoring period, temperature varied in a wide range of about -10°C to 45°C; and several events have occurred such as typhoons and asphalt pavement installation.



Fig. 1 Hwamyung cable-stayed Bridge

Table 1. Experiment History on the Hwamyung Bridge

Period	Work Phase	Description	Event
May 2011	Design sensor system	-Sensor hardware design -Operation software design	-
June 2011	Sensor system set-up	-Sensor deployment -Internet-based remote sensing setup	-
June - July 2011	Performance evaluation	-Wireless communication test -Solar power harvesting evaluation -Response signal measurement	Typhoon Maeri (June 2011)
Aug. 2011 ~ June 2013	Long-term monitoring	-Modal analysis & system identification -Cable-anchorage monitoring via vibration/impedance signals -Monitoring under temperature variation -Effect of dead load -Bridge behavior under typhoons	-Asphalt pavement (Feb. 2012) -Typhoons Bolaven, Tembin and Sanba (Aug.-Sep. 2012)

2.1 Design of wireless sensor nodes

For SHM of cable-stayed bridges, a multi-scale vibration sensor node on Imote2 platform was designed as schematized in Fig.2. The high-performance sensor platform, Imote2, provided by Memsic Co. (2010) was selected to control the operation of the sensor node. For vibration monitoring, the SHM-A and SHM-H sensor boards developed by University of Illinois at Urbana-Champaign (UIUC) (Rice et al. 2010, Jo et al. 2010) were used. The SHM-AS sensor board was modified from SHM-A sensor board in order to measure PZT's dynamic strain signal. As also shown in Fig.2, the solar-powered energy harvesting is implemented by employing solar panel and rechargeable battery. Figure 3 shows a prototype of the multi-scale sensor node which consists of three layers as 1) X-bow battery board, 2) Imote2 sensor platform, and 3) SHM-H board or SHM-A (AS) board.

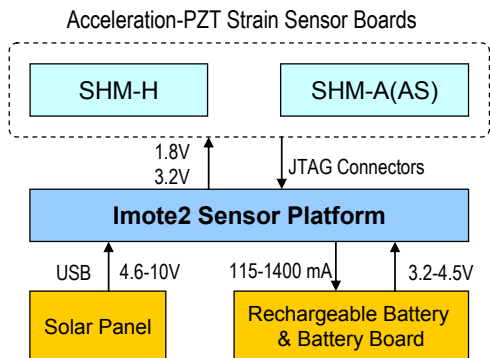


Fig. 2. Schematic of multi-scale sensor node

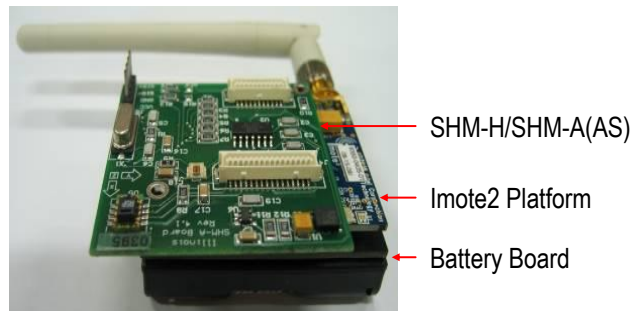


Fig. 3 Prototype of multi-scale sensor node

The Imote2 platform is built with 13-416 MHz PXA271 XScale processor (Memsic Co. 2010). This processor integrates with 256 kB SRAM, 32 MB flash memory and 32 MB SDRAM. It also integrates with many I/O options such as 3×UART, I2C, 2×SPI, USB host, GPIO. Therefore, Imote2 platform is very flexible in supporting different sensor types, analog-to-digital converter (ADC) chips and radio options. A 2.4 GHz surface mount antenna which has a communication range of about 30 m is equipped for each Imote2 platform. In order to deal with power supply issue, especially for long-term operation of smart sensor nodes, energy harvesting is essential. Due to the requirement for solar panel integrated with Imote2 such as output voltage range 4.6~10 V and output current range 115~1400 mA, SPE-350-6 solar panel (9 V, 350 mA) provided by SolarMade is selected for harvesting the solar energy.

For deck's responses, the SHM-H sensor board which includes several key components such as accelerometer, anti-aliasing filter and ADC is utilized. It employs a SD1221L-002 accelerometer for high-sensitivity channel, which has an input range of ± 2 g, a sensitivity of 2 V/g and an output noise of $5 \mu\text{g}/\sqrt{\text{Hz}}$. For cable's acceleration measurement, the SHM-A employs the tri-axial LIS344ALH accelerometer of which its sensitivity is relatively lower and output noise is quite higher than the SHM-H. In this study, a modified SHM-AS sensor board was designed to measure PZT's dynamic strain signals. The external channel (i.e., channel 4) on SHM-A sensor board is hooked up for measuring the analog signal which is processed by the ADC.

2.2 Sensor deployment on the Hwamyung Bridge

The Hwamyung cable-stayed Bridge consists of three spans including a 270-m central main span between two pylons and two 115-m side spans connecting east and west approaches. The clearance of the deck is 14.7 m from the water level. The height of two pylons is 65-m from deck level. The box girder supported by single plane stayed-cable is 27.8 m in width and 4 m in height. The bridge has total 72 cables, positioning 18 cables at one side of pylon. For the wireless SHM system on the bridge, two hardware configurations of Imote2-based smart sensor nodes which are gateway nodes and leaf nodes are designed as shown in Fig. 4. A gateway node consists of an Imote2 platform with 2.4 GHz antenna, an IBB2400 interface board connected to the PC via USB cable. A leaf node consists of an Imote2 platform with 2.4 GHz antenna, a

sensor board (e.g., SHM-AS or SHM-H), an X-bow battery board powered by a Powerizer Li-ion polymer rechargeable battery with a solar panel.

As shown in Fig. 4, 12 sensor nodes including 11 leaf nodes and 1 gateway node (i.e., gateway vibration) were installed. Among the leaf nodes, 6 Imote2/SHM-H sensors were placed at five locations of the deck and at the top of the west pylon (i.e., D1~D5, and P1), and 5 Imote2/SHM-AS sensors were placed on five selected cables (i.e., C1~C5). For each sensor board (i.e., SHM-H or SHM-AS), three axes accelerations were measured. A spared channel in SHM-AS sensor board was used for measuring dynamic strain in cable. Also for dynamic strain measurement, five PZT patches were bonded on aluminum tubes covering the five selected cables. The vibration signals were measured in duration 600 seconds with sampling rate 25 Hz.

All sensor nodes and base station are placed in plastic boxes which have waterproof rubber gaskets, as shown in Fig. 5, to prevent them from sun-heating, absorbent, and other damage caused by harsh environmental condition such as rain, wind, and dust at the field site. Solar panels were mounted on the sensor boxes to harvest the solar energy for recharging the Li-ion polymer batteries embedded to the sensor boards. A webcam was installed on the west pylon to observe the bridge's condition in real-time. A commercial 4G modem is implemented to connect the in-situ PC to internet so that the SHM system can be controlled remotely from the laboratory.

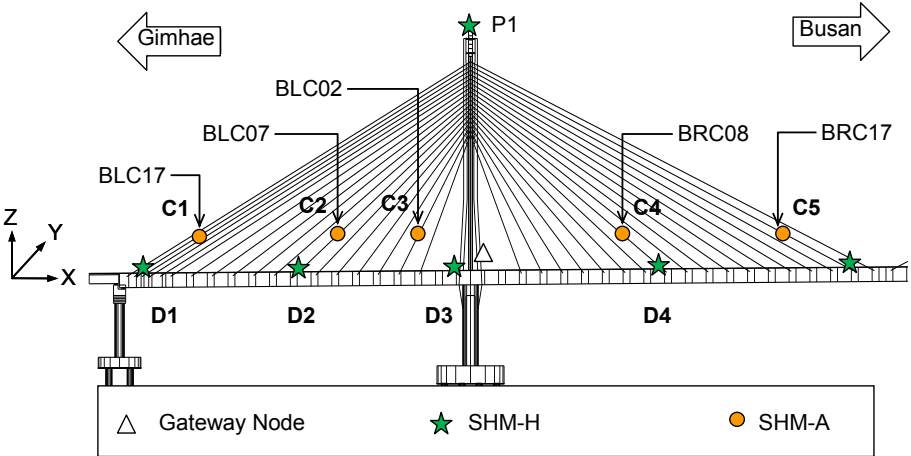


Fig. 4 Sensor layout on the Hwamyung cable-stayed Bridge

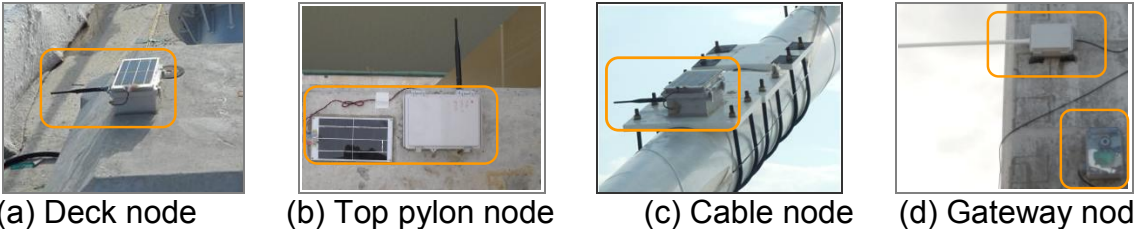


Fig. 5 Field deployment of smart sensor nodes on Hwamyung Bridge

3. LONG-TERM MONITORING

Responses of the bridge were measured by smart sensor nodes with *AutoMonitor* with two-hour interval under ambient vibration condition. Figure 6 shows examples of the power spectral densities extracted from the acceleration signals of the sensors on the pylon, the deck and the cables (i.e., sensor nodes P1, D2 and C4) under normal condition (without vehicle traffic on the bridge). Nevertheless of this low excitation condition, natural frequencies of the bridge components can be well determined, which guarantees a reliable modal identification. Note that there are unexpected periodic peaks (i.e., 0.8 Hz, 1.6 Hz) in the frequency responses of deck D2 as shown in Fig. 6(b). It has been reported that these noise peaks may be caused by the power supply issue of the SHM-H sensor board (Jo et al. 2010).

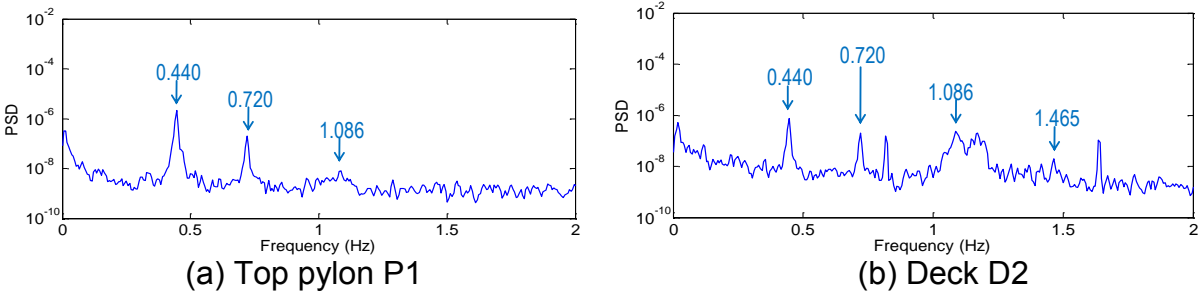


Fig. 6 Frequency responses from sensors on pylon, deck and one cable

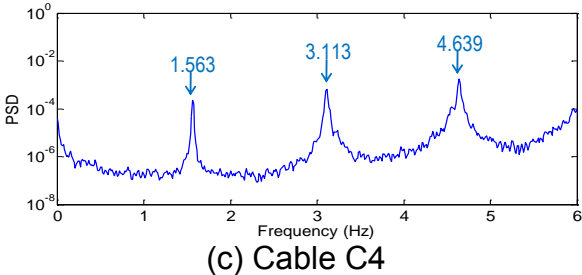


Fig. 6 Frequency responses from sensors on pylon, deck and one cable

3.1 Modal parameter identification of deck-pylon

In order to extract experimental natural frequencies and mode shapes of the deck and the pylon, the SSI method (Overschee and De Moor 1996) was utilized. The SSI method extracts the singular value decomposition (SVD) of a block Hankel matrix with cross correlation matrix of responses as follows:

$$\mathbf{H} = [\mathbf{U}_1 \quad \mathbf{U}_2] \begin{bmatrix} \Sigma_1 & 0 \\ 0 & 0 \end{bmatrix} \begin{bmatrix} \mathbf{V}_1^T \\ \mathbf{V}_2^T \end{bmatrix} \approx \mathbf{U}_1 \Sigma_1 \mathbf{V}_1^T \tag{1}$$

where \mathbf{H} is the Hankel matrix; \mathbf{U} , \mathbf{V} are the unitary matrices; and Σ_1 is the singular value matrix. The modal parameters can be identified from a system matrix which is determined from the SVD algorithm. A stabilization chart is used to find a suitable system order with the criteria which classify a mode as stable mode, unstable mode,

and noise mode (Yi and Yun 2004). Once the stable modes are detected, damping ratio (ξ_i) of the i^{th} mode is identified from the eigenvalue (λ_i) as follows:

$$\xi_i = \frac{-\text{Re}(\lambda_i)}{|\lambda_i|} \tag{2}$$

Using the SSI method, modal parameters for the first six vertical and lateral bending modes (i.e., V1~V6 and L1~L3) were extracted as shown in Fig. 7 and as listed in Table 2. Note that the experimental mode shapes are well agreed with those of a finite element analysis from Ho et al. (2012).

Table 2 Identified natural frequencies and damping ratios

	Vertical modes						Lateral modes		
	V1	V2	V3	V4	V5	V6	L1	L2	L3
Natural Freq.	0.444	0.720	1.028	1.084	1.171	1.462	0.454	0.666	1.169
Damping ratio	0.004	0.009	0.025	0.006	0.028	0.008	0.012	0.011	0.026

* Symbol L indicates lateral mode, symbol V indicates vertical mode.

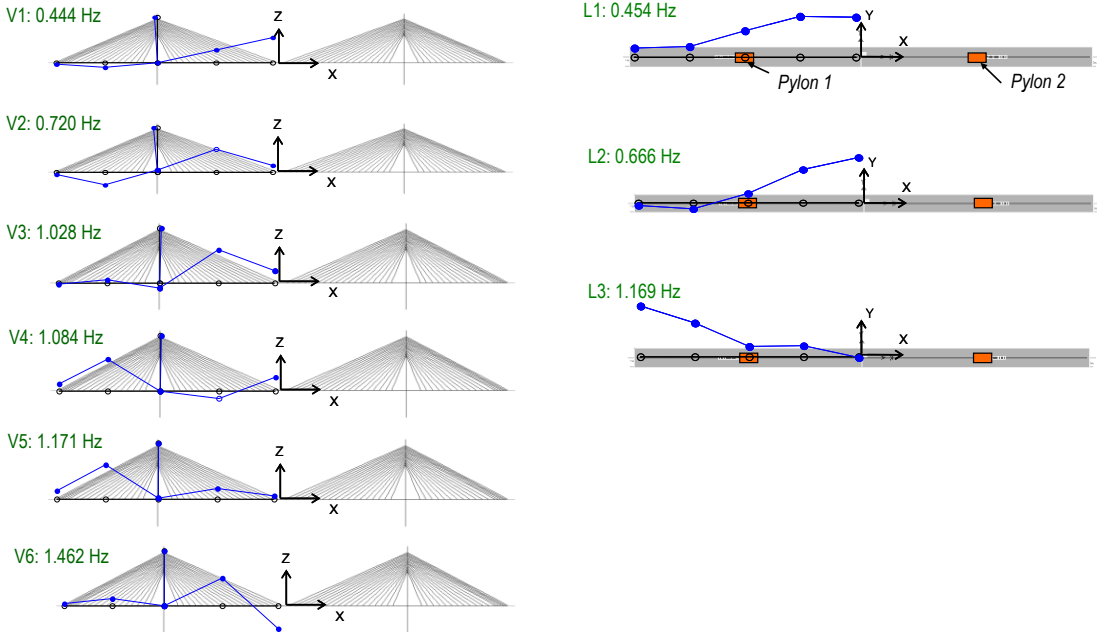


Fig. 7 Identified mode shapes of the Hwamyung Bridge

3.2 Monitoring of cables

3.2.1 Cable force estimation

The techniques to estimate cable force are classified into static and vibration-based methods. In the static method, cable force is directly measured by a load cell or a hydraulic jack. In the vibration-based method, cable force is indirectly estimated from measured natural frequencies. In practice, the vibration-based method is more widely used than the static method due to its simplicity in test procedure (Kim and Park 2007). Among available vibration-based methods (Clough and Penzien 1993, Shimada 1995,

Zui et al. 1996), the method proposed by Zui et al. (1996) is selected in this study to estimate the cable forces. The merit of this method is that the effects of both flexural rigidity and cable-sag are considered in the estimation of cable tension force so that the accuracy of the estimation can be greatly improved. For the cables in the Hwamyung Bridge, the two following formulas (out of seven original ones) are used to estimate the values of cable forces:

$$T = 4m(f_1L)^2 \left[1 - 2.2n \frac{C}{f_1} - 0.55n \left(\frac{C}{f_1} \right)^2 \right]; \quad \Gamma \geq 3; \xi < 17 \quad (3)$$

$$T_n = \frac{4m}{n^2} (f_nL)^2 \left[1 - 2.2n \frac{C}{f_n} \right]; \quad \xi \geq 200 \quad (4)$$

where T_n is the tension force by the n^{th} vibration mode; m is the mass of cable per unit length; L is the length of cable; f_1 , f_n are respectively the natural frequencies corresponding to the first and the n^{th} mode ($n \geq 2$); ξ is the parameter determined from cable properties and design conditions, $\xi = \sqrt{(T/EI)} \times L$; $C = \sqrt{(EI/mL^4)}$; and EI is the flexural rigidity of cable.

The natural frequencies of the five selected cables C1-C5 are extracted by the SSI method and utilized for cable force estimation by using Eqs. (3)-(4). The estimation results are shown in Fig. 8 together with the design forces and the lift-off test results. It is found that the vibration-based estimation results are much different from the design forces by about 0.4 - 10.3 (%). On the other hand, relatively smaller difference (about 1.1 - 6.3 (%)) is observed between the estimations and the measures from the lift-off test. It should be noted that the lift-off test results may represent the true cable tension forces at the time of the test. However, the lift-off test was carried out in December 2010 which was 6 months before the vibration test (June 2011). Hence, the estimated cable tension forces in this study could be considered as the most updated data.

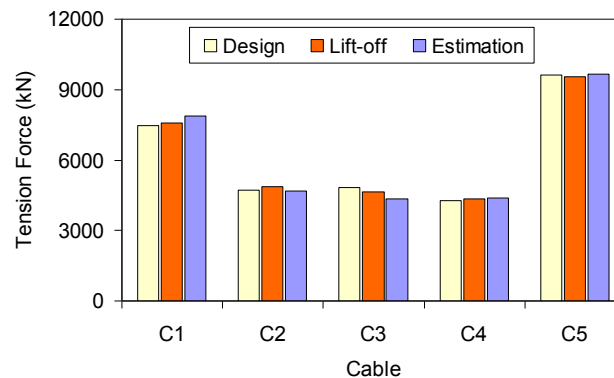


Fig. 8 Cable force estimation: Cables C1-C5

3.2.1 Effect of temperature variation on cables' natural frequencies

For a stay cable subjected to two different temperatures, the axial extension of the cable due to temperature variation (e.g., $\Delta L_T = \alpha_T L \Delta T$) is equivalent to the deformation by the change in tension force at anchorage (e.g., $\Delta F = -EA \Delta L_T / L = -\alpha_T EA \Delta T$); where

α_T is the coefficient of linear thermal expansion of the cable, ΔT is the temperature variation, and EA is the axial rigidity of the cable. The change in tension force can be simplified in a reduced order as:

$$\Delta F \approx g(m, L) \Delta f_k^2 / k^2 \quad (5)$$

where $\Delta f_k^2 = f_k^{*2} - f_k^2$ is the change in square of natural frequency; f_k and f_k^* is the k^{th} natural frequencies of the cable before and after tension force change, respectively; k is the mode number; and $g(m, L)$ represents geometric and material quantities of the cable. Hence, the change in square of natural frequency due to temperature variation is expressed as follows:

$$\Delta f_k^2 \approx -\beta_k \Delta T \quad (6)$$

where β_k is temperature correlation index which may be calculated as: $\beta_k = \alpha_T EA k^2 / g(m, L)$. Since it is difficult to obtain the geometric and material quantities $g(m, L)$ theoretically, the value of β_k can be estimated from field experiment by correlating the change in natural frequency and temperature variation.

According to the formulas of Zui et al. (1996), the first natural frequency was monitored for the short cables C2, C3 and C4, and the second natural frequency was monitored for the long cables C1 and C5. Figures 9 and 10 show the changes in the natural frequencies (corresponding to the first or the second mode dependent on cables) versus temperature change in 5 days. It is obvious that the natural frequencies change oppositely with temperature variation. This implies axial stress of the cable is partially released when temperature increases and vice versa.

The data in longer period of one month from August to September, 2011 was utilized to construct the relationship between the natural frequencies and temperature. Figures 11 and 12 illustrate the correlations between natural frequencies and temperature. It is found that the change in the cables' natural frequencies seems to be linear with temperature variation. Those monitoring results are consistent with the analytical model of temperature variation effect on change in cables' natural frequencies (Eq. 6).

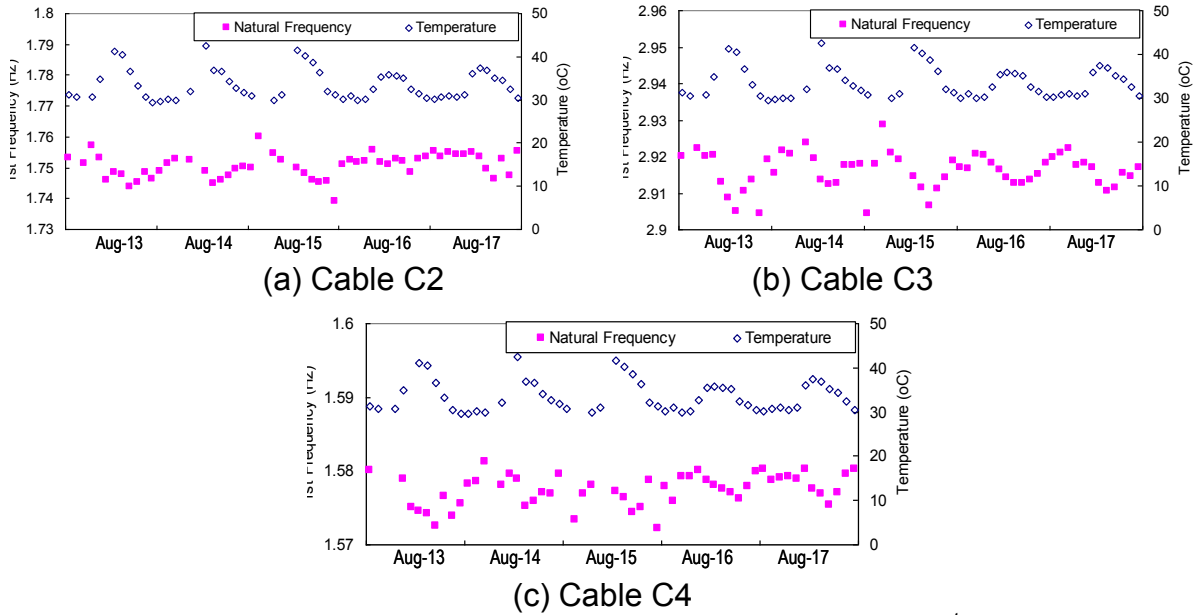


Fig. 9 Monitoring results for short cables C2, C3 and C4 in 5 days: 1st natural frequency

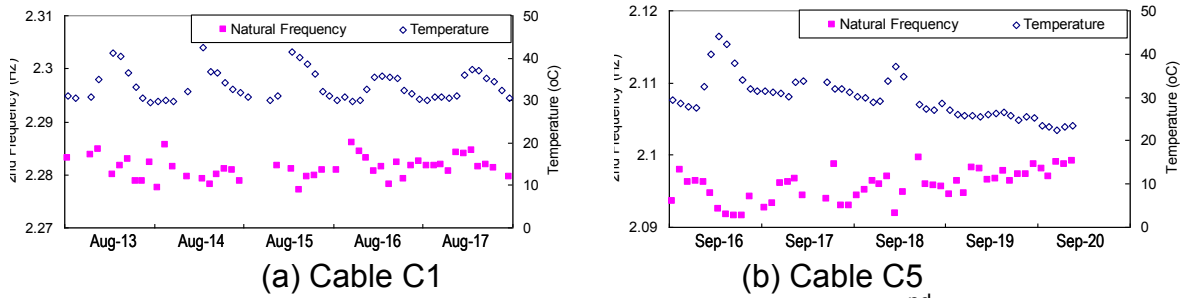


Fig. 10 Monitoring results for long cables C1 and C5 in 5 days: 2nd natural frequency

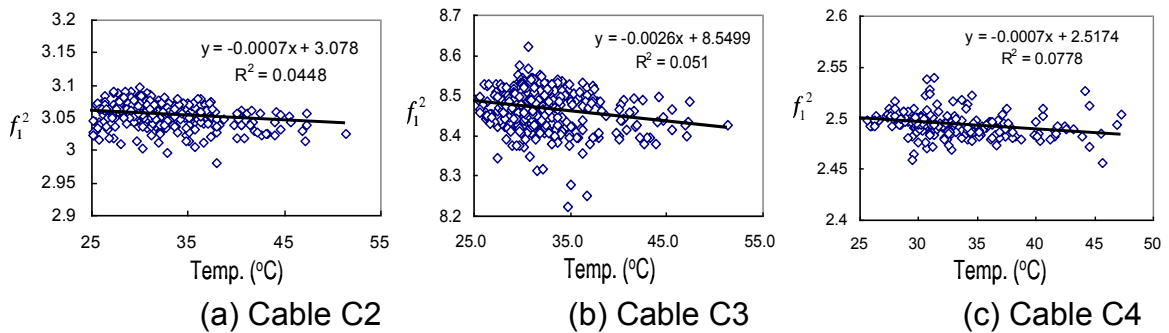


Fig. 11 Correlation of natural frequency and temperature for short cables C2, C3 and C4

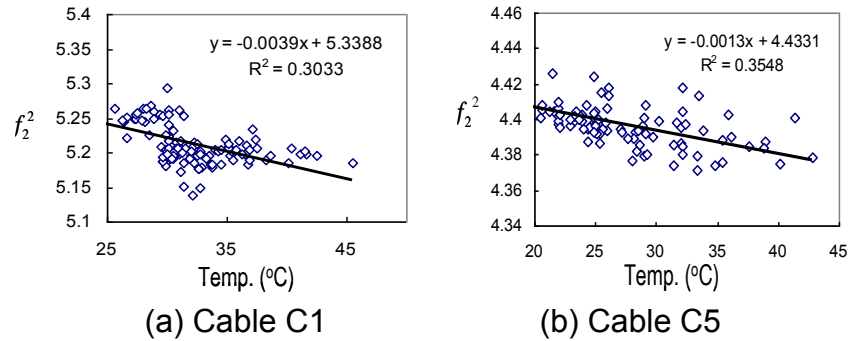


Fig. 12 Correlation of natural frequency and temperature for long cables C1 and C5

3.3 Bridge behavior under typhoon condition

Over 3 years monitoring, there were 4 typhoons passing the Korean peninsula and directly affected the site of Hwamyung Bridge, including typhoons Maeri (in June 2011), Bolaven (in August 2012), Tembin (in August 2012) and Sanba (in September 2012). During typhoon Sanba, the highest wind speed was recorded on-site as 17.9 m/s. Figure 13 show the time-frequency analysis of acceleration signals from deck D2 and cable C3 during typhoon Sanba. It is observed that the magnitudes of all vibration modes increase significantly in the period of the typhoon. This implies that the typhoon produced the impact in a wide frequency range. Also, as shown in Fig. 14, the maximum acceleration magnitude during the typhoon was much larger than those in normal wind condition. From those observations, it is found essential to have a monitoring system for the internal forces of the bridge components during typhoons.

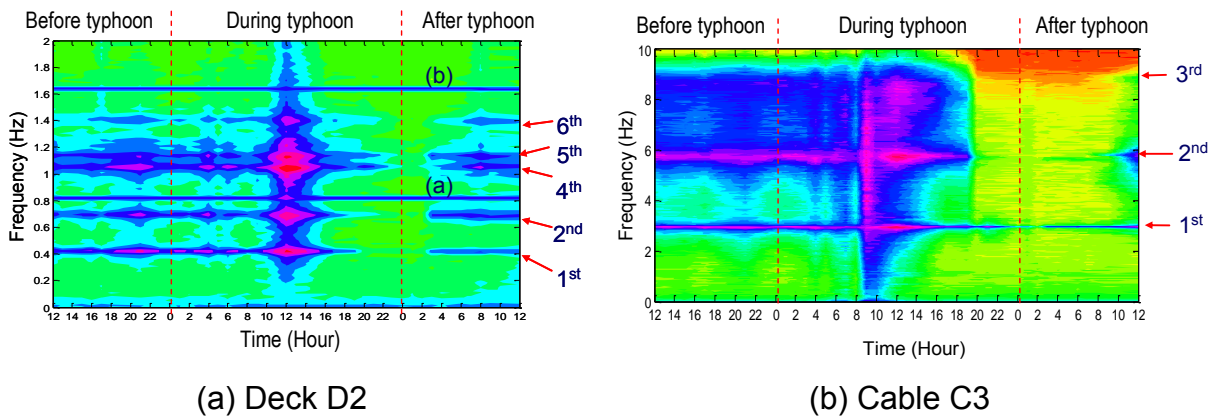
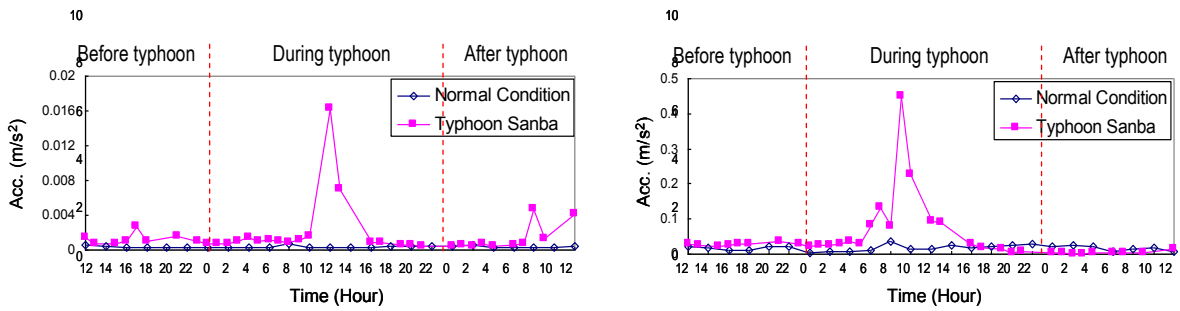


Fig. 13 Time-frequency acceleration response of deck and cable during typhoon Sanba



(a) Deck D2 (b) Cable C3

Fig. 14 Maximum acceleration of deck and cable during typhoon Sanba

3.4 Effect of dead load variation

The changes in natural frequencies were examined after the asphalt pavement was laid on the bridge on February, 2012. The data of two time periods with similar temperatures, August 2011 and August 2012 (as shown in Fig. 15), were analyzed. Figure 16 shows the measured natural frequencies of the first mode of the deck and cable C3 at the two periods. It is found that that the natural frequency of deck decreased after laying the pavement, whereas the natural frequency of the cable increased after laying the pavement. These phenomena can be explained by the following reasons: the mass of deck was increased due to the pavement's mass, and the tension force of the cable was also increased due to the additional supported load from the weight of the deck.

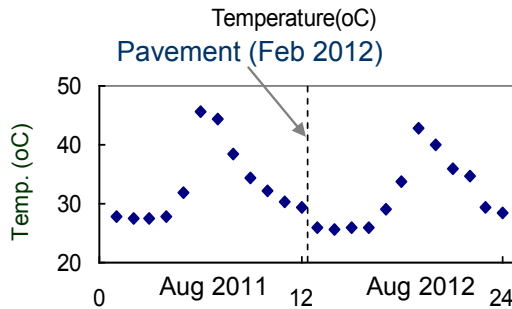
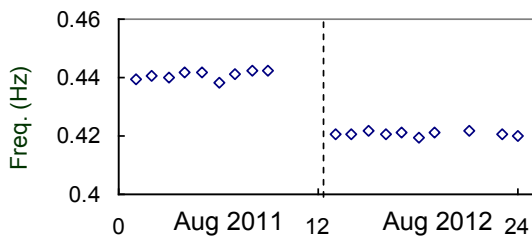
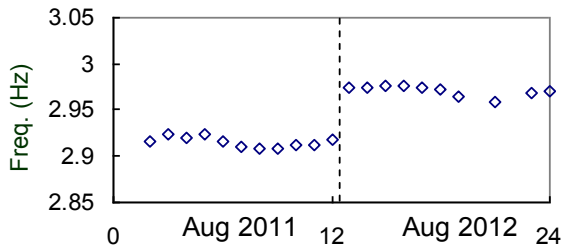


Fig. 15 Temperature before and after asphalt pavement
Deck: First Frequency (Hz) Cable C3: First Frequency (Hz)



(b) 1st frequency of deck



(c) 1st frequency of cable C3

Fig. 16 Changes in natural frequencies before and after asphalt pavement

4. CONCLUSIONS

This paper presented the long-term monitoring of the Hwamyung cable-stayed Bridge in Korea using an Imote2-platformed WSN. First, the wireless monitoring system of the bridge was briefly described. Next, modal parameters of the bridge and cable forces of several selected cables were estimated from the acceleration signals measured by the WSN. It was found that the experimental modal parameters of the bridge were well matched with those of a finite element analysis. Also, the cable forces were found close to the forces as installed. Then the effects of environmental and loading factors on the bridge's characteristics were experimentally investigated. It has been found that the square of the cable natural frequencies was varied linearly to temperature variation. Natural frequencies of the deck and the cables were much influenced by dead load variation, but in opposite trends. During the typhoons observed on the bridge, the vibration amplitudes of the deck and the cables significantly increased, and all extracted modal response became more resonant.

ACKNOWLEDGEMENT

This work was supported by Basic Science Research Program through the National Research Foundation of Korea (NRF) funded by the Ministry of Education, Science and Technology (2011-0004253)

REFERENCES

- Doebling, S.W., Farrar, C.R., and Prime, M.B. (1998), "A summary review of vibration-based damage identification methods", *The Shock and Vibration, Digest*, Vol. 30(2), 1998, 91-105.
- Clough, R.W., and Penzien, J. (1993), *Dynamics of structures*, Second Edition, McGraw-Hill.
- Ho, D.D., Lee, P.Y., Nguyen, K.D., Hong, D.S., Lee, S.Y., Kim, J.T., Shin, S.W., Yun, C.B., and Shinozuka, M. (2012), "Solar-powered multi-scale sensor node on Imote2 platform for hybrid SHM in cable-stayed bridge", *Smart Structures and Systems*, Vol. 9(2), 145-164.
- Jo, H., Rice, J.A., Spencer, B.F., and Nagayama, T. (2010), "Development of a high-sensitivity accelerometer board for structural health monitoring", *Proc. of the SPIE*, San Diego, USA.
- Kim, B.H., and Park, T. (2007), "Estimation of cable tension force using the frequency-based system identification method", *Journal of Sound and Vibration*, Vol. 304, 660-676.
- Kim, J.T., Park, J.H., Hong, D.S., and Park, W.S. (2010), "Hybrid health monitoring of prestressed concrete girder bridges by sequential vibration-impedance approaches", *Engineering Structures*, Vol. 32, 115-128.
- Kim, J.T., Park, J.H., Hong, D.S., and Ho, D.D. (2011), "Hybrid acceleration-impedance sensor nodes on Imote2-platform for damage monitoring in steel girder connections", *Smart Structures and Systems*, Vol. 7(5), 393-416.
- Lynch J.P., Wang, W., Loh, K.J., Yi, J.H., and Yun, C.B. (2006), "Performance monitoring of the Geumdang bridge using a dense network of high-resolution wireless sensors", *Smart Materials and Structures*, Vol. 15, 1561-1575.

- Mascarenas, D.L., Todd, M.D., Park, G., and Farrar, C.R. (2007), "Development of an impedance-based wireless sensor node for structural health monitoring", *Smart Materials and Structures*, Vol. 16, 2137-2145.
- Memsic Co. (2010), "Datasheet of ISM400", Available at <http://www.memsic.com>.
- Overschee, V.P., and De Moor, B. (1996), "Subspace identification for linear system", Kluwer Academic Publisher.
- Rice, J.A., Mechitov, K., Sim, S.H., Nagayama, T., Jang, S., Kim, R., Spencer, Jr, B.F., Agha, G., and Fujino, Y. (2010), "Flexible smart sensor framework for autonomous structural health monitoring", *Smart Structures and Systems*, Vol. 6(5-6), 423-438.
- Shimada, T. (1995), "A study on the maintenance and management of the tension measurement for the cable of bridge", *Ph.D. Dissertation*, Kobe University, Japan.
- Sohn, H., Farrar, C.R., Hemez, F.M., Shunk, D.D., Stinemates, D.W. and Nadler, B.R. (2003), "A review of structural health monitoring literature: 1996-2001", *Los Alamos National Laboratory Report*, LA-13976-MS, Los Alamos, NM.
- Spencer, B.F., and Cho, S. (2011), "Wireless smart sensor technology for monitoring civil infrastructure: technological developments and full-scale applications", *Proc. of ASEM'11 Plus*, Seoul, Korea.
- Straser, E.G., and Kiremidjian, A.S. (1998), "A modular, wireless damage monitoring system for structure", *Technical Report 128*, John A. Blume Earthquake Engineering Center, Stanford University, Stanford, USA.
- Yi, J.H., and Yun, C.B. (2004), "Comparative study on modal identification methods using output-only information", *Structural Engineering and Mechanics*, Vol. 17(3-4), 445-446.
- Zui, H., Shinke, T., and Namita, Y. (1996), "Practical formulas for estimation of cable tension by vibration method", *Journal of Structural Engineering*, Vol. 122(6), 651-656.